Proceedings of Ninth World Conference on Earthquake Engineering
August 2-9, 1988, Tokyo-Kyoto, JAPAN (Vol.III)

4-3-22

A SIMULATION STUDY OF GROUND LIQUEFACTION IN A SOIL-STRUCTURE INTERACTION PROBLEM

Tadahiko SHIOMI[1], Shoichi TSUKUNI[2] and Yoshiyuki TANAKA[2]

[1] Technical Research Laboratory, Takenaka Corp.
Koto-ku, Tokyo, Japan
[2] Engineering Department, Takenaka Doboku Co., Ltd.
Chuo-ku, Tokyo, Japan

SUMMARY

Simulation analysis of ground liquefaction is an urgent requirement for recent seismic engineering. In order to respond to the requirement, we introduced an approach to the dynamic effective analysis in a program called DIANA and demonstrated its capabilities. The full two phase dynamic equation was adopted so that the approach can simulate re-distribution of pore pressure. The constitutive models of the reflecting surface model and the Pastor-Zienkiewicz model were studied with the approach. The approach was verified by simulation of shaking table tests. The numerical and experimental results showed good agreement.

INTRODUCTION

Prediction of ground liquefaction is of prime importance in earthquake engineering for sandy soil ground. Extensive researches since the Niigata earthquake in 1964 made possible estimation of liquefaction potential. Re-distribution of pore pressure, however, was neglected in the estimation. In reality the generated and accumulated pore pressure can be transferred to the most critical location in strength. This transfer might have caused the failure of the Lower San Fernando Dam which took place after the earthquake excitation had finished. To solve this type of problem, a finite element method based on the two phase theory with elasto-plastic theory (Ref.1,2) has been implemented in the DIANA program (Dynamic Interaction Approaches and Nonlinear Analysis). Theoretical back grounds are summarized in this paper. We report one of the verification studies of the approach which is a simulation analysis of a shaking table test of a soil-structure problem. Determination of the soil constants are a critical part of the analysis. So some laboratory tests were conducted in addition to conventional approaches.

THEORY AND NUMERICAL PROCEDURE

The two phase dynamic equation proposed for the porous saturated material with ground water was adopted. The formulation describes the interaction behavior of the soil skeleton and pore water by the Darcy's law. This phenomena represent the dissipation of pore water pressure. The generation of pore water pressure is modeled by the constitutive equations which should be able to represent the dilatancy effect. Among many constitutive equations, the reflecting surface model and the Pastor-Zienkiewicz model are reported.

General Formulation for Two Phase Continua The governing equations were derived as follows assuming small deformation of solid and small flow of the fluid and negligence of the convective term.

$$\sigma'_{ji,j} - (1-n)p_{,i} + (1-n)\rho_s b_i + (1-n)\rho_s \ddot{u}_i + \dot{w}_i/k = 0 \qquad (1)$$

$$-np_{,i} + n\rho_f b_i - n\rho_f \ddot{U}_i - \dot{w}_i/k = 0 \qquad (2)$$

where σ'_{ij} is the effective Cauchy stress of a solid at any instant, ρ_s and ρ_f are the density of the soil particles and the fluid itself respectively. u_i and U_i are the displacements of the solid skeleton and fluid respectively, p is the pore pressure and b_i is a body force. "." denotes the time derivative. k is the Darcy's permeability coefficient. n denotes porosity of the soil.

Finite Element Formulation Generic discretized formulation of the two phase media for compressive fluid with Eqs. (1) and (2) are derived as

$$\int_\Omega N^u_{k,j}\sigma_{ij}d\Omega + \mathbf{K}_1\bar{u} + \mathbf{K}_2\bar{U} - \mathbf{C}_2\dot{\bar{U}} + \mathbf{C}_1\dot{\bar{u}} + \mathbf{M}_s\ddot{\bar{u}} = \bar{f}_s \qquad (3)$$

$$\mathbf{K}_2\bar{u} + \mathbf{K}_3\bar{U} - \mathbf{C}_2\dot{\bar{u}} + \mathbf{C}_3\dot{\bar{U}} + \mathbf{M}_f\ddot{\bar{U}} = \bar{f}_f$$

where N is the shape function, $\mathbf{M}$, $\mathbf{C}$ and $\mathbf{K}$ are mass, damping and stiffness matricies.

Soil Models we chose two soil models for the comparative studies.

a. Reflecting Surface Model(R-S model: Ref.3) The model was proposed by Pande and Pietruszczak. A single mechanism of f and g and the hardening parameter H_p are defined as

$$f = g = \sigma_m'^2 + 2\sigma_m' a + \frac{\bar{\sigma}^2}{g(\theta)^2} = 0, \qquad H_p = \frac{\partial f}{\partial a}\cdot\frac{\partial a}{\partial e^p}\cdot\frac{\partial g}{\partial \sigma_{ij}}\delta_{ij} \qquad (4)$$

The same functions f and g are chosen for both the loaded and unloaded cases. The variable "a" is a size parameter of yield and potential function. The incremental form of "a" is defined in Eq.(5) as a function of the current stress point in the e-log(σ_m) curve.

$$\frac{\partial \ln(a)}{\partial e^p} = \left(\frac{1}{W_1} - \frac{1}{W_2}\right) e^{z(e^p - e^p_o)} - \frac{1}{W_1} \qquad (5)$$

where W_1 and W_2 is the slope of the plastic specific volume e^p against the logarithmic mean stress σ'_m.

b. Pastor-Zienkiewicz Model(P-Z model: Ref.4) The potential surface is defined as a function of dilatancy as follows.

$$\frac{\partial g}{\partial \sigma_{ij}} = \frac{1}{1+d_g^2}\frac{\partial \sigma_1}{\partial \sigma_{ij}}\{1, d_g\}, \text{ where } d_g = (1+\alpha_g)(M_g - \eta) \qquad (6)$$

where α_g and M_g are material constants. Its yield function is defined using the same form of the potential function by introducing the material constants α_f and M_f. α_f is assumed equal to α_g in most cases. The hardening parameter H_p is defined for loaded and unloaded processes independently. For the loaded case,

$$H_p = H_o\,\sigma_m'^n\{1-\frac{\eta}{\eta_f}\}^4\{1 - \frac{\eta}{M_g} + \beta_o\beta_1\exp(-\beta_o\xi)\}$$

For the unloaded case,

$$H_p = H_{uo}\{\frac{\eta_u}{M_g}\}^{-\gamma_u} \qquad (7)$$

ξ is the equivalent strain, β_0, β_1, n, H_0, H_{uo} and γ_u are additional soil constants, η is the stress ratio and η_f is the maximum stress ratio.

VERIFICATION STUDY - TRIAXIAL TEST

A Triaxial Test A series of triaxial tests have been simulated by the two soil models. In the triaxial test, cyclic axial stress $\sigma_c + \sigma_d$ was applied to the

specimen through a load cell where σ_c is a constant confining pressure and σ_d is a dynamic part of the stress. The stress in a radial direction was kept to the constant confining pressure σ_c. The deviatoric stress was equal to σ_d and the total mean stress σ_m was $\sigma_c + \sigma_d/3$. The pore pressure p was measured through the bottom of the specimen. Then the effective mean stress was calculated as $\sigma_m' = \sigma_c + \sigma_d/3 - p$.

Determination of Soil Constants Clean Toyoura sand was used in the test. The specific gravity was 2.65, and the maximum and minimum dry density of the sand were 1.648 and 1.356 g/cm³ respectively. Elastic modula were derived from the first cycle of the test. The internal friction angle, Φ_d, of the sand was determined from the experimental equation (Eq. 8) based on the triaxial compression tests under a consolidated drained condition using Toyoura sand (Ref.5).

$$\Phi_d = 32.5 + 20.6\,(D_r - 40) / 100 \qquad (8)$$

where D_r denotes the relative density of the soil layer in percentage.

Table 1 Material properties

K_0 = 598 kg/cm², G_0 = 230 kg/cm² at 0.5kg/cm², Failure angle=37.5°.
For R-S model: λ = 0.016575, k = 0.00453, β = 0.018.
P-Z model: M_f = 0.68, α_f = 0.35, β_0 = 4, M_g = 1.2, α_g = 0.35, β_1 = 0.2, H_0 = 9000, H_{U0} = 6000.

Remarks of Simulation Results The accumulation of excess pore pressure (e.p.p.) is shown in Fig. 1. The curve of the measured e.p.p shows a slight curve upward as shown. But the e.p.p envelope of the P-Z is concave. The results of the simulation and experiments showed reasonable agreement.

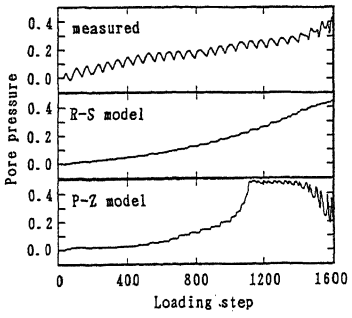

Fig. 1 History of Excess Pore Pressure

Stress strain relationships are shown for axial stress in Fig. 2. The simulation results are good at the average slope of the diagram but none of them reproduced good hysteresis loops. Dependency on stiffness in the mean stress were seen in the both the measurement and calculations.

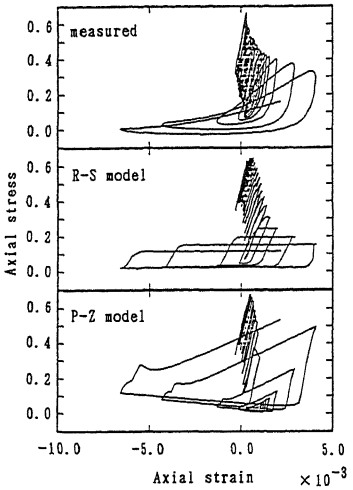

Fig. 2 Stress Strain Curve

VERIFICATION STUDY - SHAKING TABLE TEST

Simulation analyses of shaking table tests are described in detail. As shown in Fig. 3, the model ground was made of saturated sand 40 cm deep and 160 cm long. A layer of coarse sand was stuck to the bottom of the box to prevent slippage between the model ground and the box. Furthermore, 5 cm thick foam rubber cushions were placed at both side boundaries as radiational boundaries. The sand used was Toyoura sand.

The models had rigid structures (20 cm long, 28 cm wide and 10 cm high) at the center of the surface of the level ground. The contact pressure of the rigid structure was 21.5 gf/cm². The soil ground was homogeneous and its relative density was 47.6 %. The initial water table was 3.3 cm deep. The pore water pressure and the horizontal

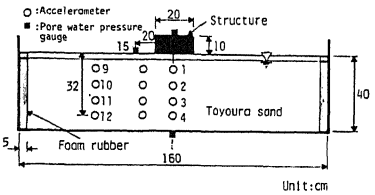

Fig. 3 Model of Shaking Table Test

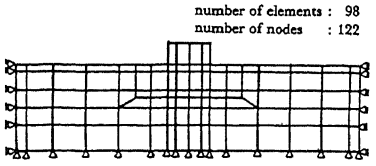

Fig. 4 Finite Element Model (Coarse Mesh)

acceleration were measured at 12 points and 3 points respectively as shown in Fig. 3.

A two dimensional numerical model is shown in Fig.4. Procedures of identifying the soil constants of the models are discussed as follows.

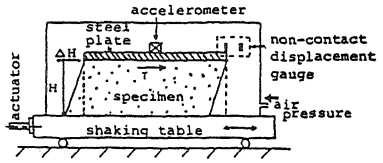

Fig. 5 Shear Modulus Test Apparatus

Material Constants The same values of the triaxial test were used for the material constants except the elastic modula(R-S model). The low confining pressure caused a significant difference in the elastic modula. The shear modulus Go was determined from the following experimental formula (Ref.6) which was obtained for the low confining pressure using the apparatus shown in Fig. 5. In this test, the shear stress was produced by the inertia force of a steel plate on the specimen (30 cm in diameter and 5 cm in height) and the confining pressure was applied by air pressure and the dead weight of the steel plate on the test specimen.

$$G_o = A\,(B - e)^2\,\sigma_m^n\,/\,(1 + e) \qquad (9)$$

where A=38.33, B=2.17, n=0.38 were used.

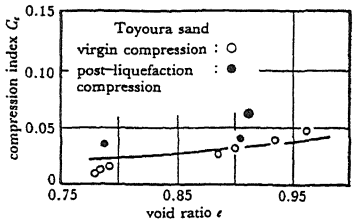

Fig. 6 Compression Index

The compression and swelling indexes are also not easy to define for the low level stress, so special consolidation tests for such low stress level were conducted to confirm the consistency of the index value to the ordinary confining pressure. Fig. 6 shows the relationship between the void ratio and the compression index. As the void ratio increases the compression index slightly increases.

Table 2 Material Properties

a. Ground

ρ_s =2.65 g/cm³, ρ_f =1.0g/cm³	
K of fluid	= 2.22*10⁵ kg/cm²
Porosity	= 0.441
Permeability	= 0.028 cm/sec
Friction Angle	= 37.2°
(for R-S model)	
Compression Index	0.01675
Swelling index	0.00452
R-S param. β	0.2
(for P-Z model)	
M_g=1.2, α_g=0.5, M_f=0.7,	
α_f=0.5, b_0=4.0, b_1=0.2,	
H_0=500, H_{u0}=100, r_u=5, r=5	

b. Structure

ρ = 2.15 g/cm³	
Young's Mod.	= 2*10⁵ Kg/cm²
Poisson's ratio	= 0.3

All the other material properties are listed for the sand and the rigid structure in Table 2. The parameters of the P-Z model had to redetermined.

Comparison between Calculations and Experiments Fig. 7 shows the input acceleration, which was observed at the bottom of the shaking box. The input motion was cyclic motion at 2 Hz and continued for 2 seconds. The maximum acceleration was 100 gal at 11.4 seconds. The calculation has done at 20 seconds which is well after the input motion finished so that the dissipation of the pore pressure was calculated.

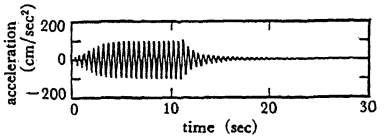

Fig. 7 Input Motion

We simulated the shaking table test by the R-S model and the P-Z model. Since the R-S model showed the better results in the triaxial simulation so that the simulation of the R-S model is reported in the first and some comments are added for the results of P-Z model.

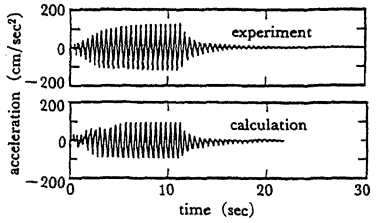

Fig. 8 Respose Acceleration (R-S Model)

a. Response Acceleration The horizontal accelerations on the top of the structure are shown in Fig. 8. The response amplitude was almost 1.0 for the results measured and calculated. That means that the natural frequency was much higher than the frequency of the input motion. The

acceleration of the calculations and the experiments showed good agreement. They *maintained good shape during the excitation and ceased when the input motion* stopped. So it is considered that full liquefaction did not take place in this test.

b. Excess Pore Pressure The time history of the excess pore pressure is shown in Figs. **9** and **10** for the R-S model and the P-Z model respectively. In both cases, the calculated results showed faster accumulation at the beginning and slower accumulation as they approached the peak.

After the excess pore pressure reached the peak, they started dissipating before the input motion stopped in the experiment. This was not observed in the numerical results except a little dissipation at the bottom layer under the rigid structure. This phenomena may be due to the strain dependency of the permeability during the earthquake excitation. In this study the permeability was assumed constant.

The maximum excess pore pressure ratios are shown in Fig. **11** for the R-S model and Fig. **12** for the P-Z model. The ratios at the center are lower than those at the free surface domain. This tendency was well simulated by the calculation except the lower layers where slight difference was observed. Error of simulation was larger for the P-Z model than for the R-S model.

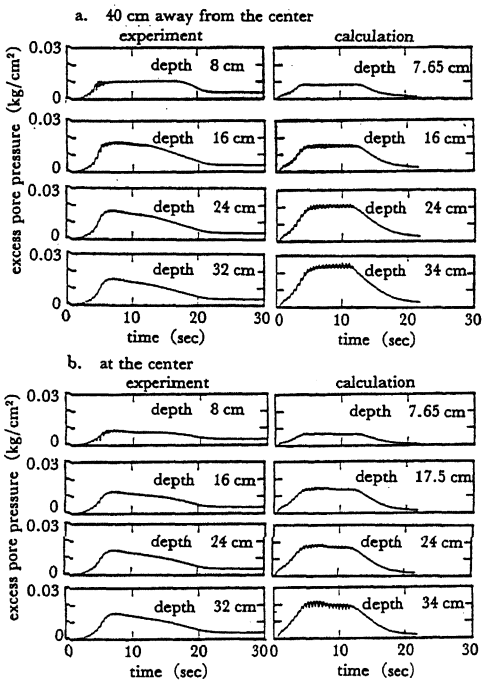

Fig. 9 Time History of Pore Pressure (R-S Model)

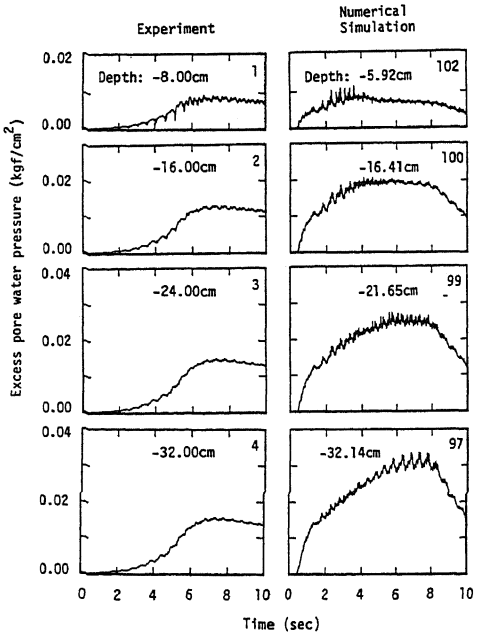

Fig. 10 Time History of Pore Pressure (P-Z Model)

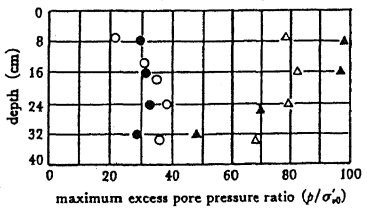

at the center
(experiment : ●
calculation : ○)
40 cm away from the center
(experiment : ▲
calculation : △)

Fig. 11 Maximum Pore Pressure Ratio (R-S Model)

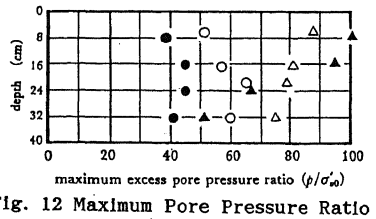

Fig. 12 Maximum Pore Pressure Ratio (P-Z Model)

c. The Settlement of the Rigid Structure The time history of the settlement of the rigid structure and the final deformation profile are shown in Figs. **13** and **14**. The settlement of experiment was 0.45cm against 0.65cm calculated by the R-S model and coarse mesh (Fig.**13**). That means the error was about 31%. This error, however, was due to mesh size and was improved by using a finer mesh. The final deformation pattern calculated by the finer mesh is shown in Fig. **14**. The final settlement was 1.8cm in the calculation against 2cm in the experiment in that case.

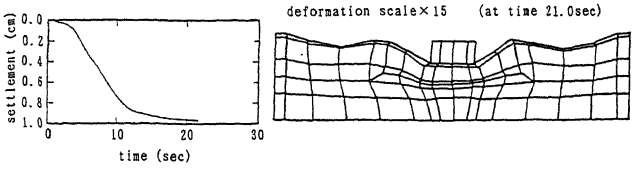

Fig. 13 Settlement of Rigid Structure (Coarse Mesh)

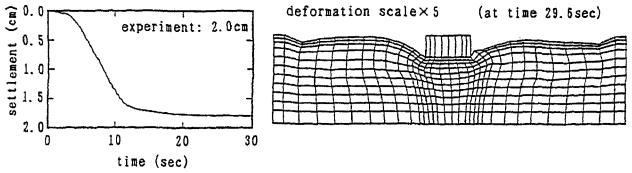

Fig. 14 Settlement of Rigid Structure (Fine Mesh)

CONCLUSIONS

Dynamic effective analysis is necessary for the analysis of sandy soil subjected to not only earthquake but also cyclic and random loading such as that caused by traffic. The dissipation process must be taken into account for the analysis where the pore water pressure generation is important. Therefore we introduced the dynamic effective stress analysis with the soil models which are capable to describe the liquefaction phenomena due to dilatancy effect. The capability of the approach and the effects of the pore water generation and dissipation are shown in the example.

The mechanisms of the liquefaction phenomena were studied through the simulation analysis on the shaking table test of the soil structure problem. The simulation capability of the soil model and the two phase analysis were demonstrated for the complex condition of the ground showing good agreement on the excess pore water pressure accumulation, response acceleration and deformation of the model ground. The comparisons of the analytical results were good for all the measured variables. Among these three measurements, the deformation was affected by the size of the finite element mesh.

The material properties were examined for the low confining pressure level. And the experimental equations and figures obtained in this study are presented.

Reference

1. Zienkiewicz, O.C. and Shiomi, T, Dynamic Behaviour of Saturated Porous Media: The Generalized Biot Formulation and Its Numerical Solution, International Journal for Num. and Anal. Methods in Geomechanics,vol 8 71-96, (1984).
2. Shiomi, T., Tsukuni, S., Hatanaka, M., Tanaka, Y., Suzuki, Y. and Hirose, T. Simulation Analysis of Ground Liquefaction Induced by Earthquake, Takenaka Technical Research Report NO. 39, pp. 101-118, (1988)
3. Pande, G. N. and Pietruszcak, S., Reflecting Surface for Soil, Proc. of Int. Sym. on Num. Models in Geomechanics, Zurich, 50-64, (1982)
4. Pastor, M. and Zienkiewicz, O. C., A Generalized Plasticity : Hierarchical Model for Sand under Monotonic and Cyclic Loading, INME report C/R/534/86, Univ. College of Swansea, (1986).
5. Hatanaka, M., Fundamental Studies on Undisturbed Sampling of Saturated Sands by Freezing, Doctor Thesis, Tokyo Institute of Technology (1977)
6. Sugimoto, M. et. al., 20th Japan National Conf. on Soil Mech. and Foundation Engng,501-502,(1983)